

ULTRAFAST LASER DIRECT WRITING OF CONDUCTIVE PATTERNS ON MODIFIED  
POLYIMIDE FILM FOR FLEXIBLE ELECTRONIC APPLICATIONS

A Thesis

by

ISHRAT JAHAN BISWAS

Submitted in Partial Fulfillment of the  
Requirements for the Degree of  
MASTER OF SCIENCE IN ENGINEERING

Major Subject: Manufacturing Engineering

The University of Texas Rio Grande Valley

December 2022



ULTRAFAST LASER DIRECT WRITING OF CONDUCTIVE PATTERNS ON MODIFIED  
POLYIMIDE FILM FOR FLEXIBLE ELECTRONIC APPLICATIONS

A Thesis  
by  
ISHRAT JAHAN BISWAS

COMMITTEE MEMBERS

Dr. Farid Ahmed  
Chair of Committee

Dr. Jianzhi Li  
Committee Member

Dr. Ali Ashraf  
Committee Member

Dr. Zhaohui Geng  
Committee Member

December 2022



Copyright 2022 Ishrat Jahan Biswas  
All Rights Reserved



## ABSTRACT

Biswas, Ishrat Jahan, Ultrafast Laser Direct Writing of Conductive Patterns on Modified Polyimide film for Flexible Electronic Applications. Master of Science in Engineering (MSE), December, 2022, 31 pp., 4 tables, 19 figures, references, 25 titles.

Conductive patterns can be printed on a flexible polymer substrate using the direct laser writing (DLW) method. In order to write conductive circuits in such polymer using a laser, polyimide (PI) is a desirable material choice due to its electrical, chemical, and mechanical properties. Electrically non-conductive PI has shown great potential for flexible printed electronics as LDW enables selective carbonization in the bulk of such material leading to the formation of conductive lines. The technique is shown to be a rapid and minimal cost method for printing electrodes to nanoscale devices. However, investigations in this field show several limitations to this strategy, such as the limited conductivity of written structures and the brittleness of carbonized PI. Therefore, more research is required to overcome those limitations and reap the benefits of the LDW approach in writing flexible electronic circuits in PI. This proposed study explores potential approaches to boost the electrical conductivity of laser written bulk carbon structures in PI films. To increase the conductivity of the carbon structure, the deposition of laser energy was adjusted by adjusting critical process parameters such as pulse energy, pulse repetition rate, and laser scan hatch distance. The experimental results demonstrate that the conductivity of carbon structures in PI films is a significant determinant of laser energy deposition. The deposition of laser energy is the most important factor as energy over the

threshold level damages the film while energy below the threshold level cannot produce carbon structure properly. In order to further increase the electrical conductivity of laser written structures, the potential of a composite film made of silver strands and PI was examined, followed by laser carbonization. Two different laser systems were used to find out the better setup for the carbonization process. Findings show a trend of improvement of conductivity of the carbonized pattern with a percentage of silver strands. The proposed LDW of conductive lines has potential in flexible electronic circuits and sensing applications.



## DEDICATION

To my parents, Shahnaj Khatun and Elias Uddin Biswas, for whom I am who I am. Also, to my sister, Nova, who backs up all my choices. Mahir Abrar, for always being by my side.



## ACKNOWLEDGMENTS

I would like to express my gratitude to my supervisor, Dr. Farid Ahmed, for his supervision. His continuous support and guidance have been invaluable to me during this journey, and I have no words to adequately thank him. I also want to express my gratitude to Dr. Jianzhi Li for his support; without him, starting at UTRGV would not have been possible. Dr. Jasim Uddin deserves special recognition for his cooperation.

A special thank you to Dr. Victoria Padilla, Cecilia Ledezma, and Salauddin Ahmed, who were kind enough to help with SEM and EDS analysis. Hernan Aparicio deserves special mention for his cooperation when I needed it.

I would also like to thank my colleagues and friends at the lab, especially Enrique and Anitha, who made my time at the lab a great experience. Enrique deserves extra special thanks because he went above and beyond during my toughest moment. I'd like to acknowledge my friends for being wonderful friends; Binti, Oishi, Piu, Sameen, Shipi, Tanu, Mahir, Lubna, Mahila, Haimanti, Sadaf, Emu, Kim, Nazim.

Lastly, I want to specifically acknowledge Dr. Samantha Lopez for her generosity at a time when I needed it most.



## TABLE OF CONTENTS

	Page
ABSTRACT.....	iii
DEDICATION.....	v
ACKNOWLEDGMENTS .....	v
TABLE OF CONTENTS .....	vii
LIST OF TABLES .....	viii
LIST OF FIGURES .....	ix
CHAPTER I. INTRODUCTION.....	1
CHAPTER II. BACKGROUND .....	4
Direct Laser Writing and Carbonization of PI .....	4
Research Question.....	5
Modification of Polyimide Film.....	6
CHAPTER III. METHODOLOGY .....	7
Material Preparation .....	7
Pure polyimide.....	7
Silver strands-polyimide composite film.....	7
Laser Processing.....	11
Ultra-fast laser carbonization.....	11
Continuous-wave laser carbonization .....	12
CHAPTER IV. RESULTS AND FINDINGS .....	14
Pulsed Laser Processed .....	14
CW-Laser Processing in Ar Gas Environment .....	22
CHAPTER V. CONCLUSION, LIMITATIONS, & FUTURE DIRECTION.....	27
REFERENCES .....	28
BIOGRAPHICAL SKETCH .....	31



## LIST OF TABLES

	Page
Table 1: Process parameters for CW laser system.....	13
Table 2: Resistance value for 1×10 mm carbonized lines at speed 10m/s and laser energy of 3μJ.....	19
Table 3: Resistance value for different numbers of laser scanning lines with hatch 25μm .....	21
Table 4: Resistance value of 1×10 mm carbonized lines at hatch distance of 0.08mm and power 10W.....	25





## LIST OF FIGURES

	Page
Figure 1: (a) Granulate PI resin. (b) 15wt.% of PI in the solvent NMP (c) Dissolving PI in the NMP at the low-speed mixer .....	7
Figure 2: (a) Polyimide resin dissolved in NMP after 24 hours of mixing at low speed. (b) Dip coating of glass slide into the PI solution. (c) Fully cured PI film .....	8
Figure 3: SEM image of silver strands .....	9
Figure 4: Image of Ag-PI composite solution for different wt.% of silver strands .....	10
Figure 5: SEM image of 5wt.% Ag-PI composite film .....	10
Figure 6: Ultrafast laser system used for carbonization .....	11
Figure 7: Femtosecond pulsed laser processed carbonized pattern by varying process parameters on different wt.% of silver-PI composite film. (a) Pure PI film. (b) (c) (d) and (e) are 0.5%, 1%, 2%, and 5% .....	14
Figure 8: Optical microscopic image of ultrafast laser processed carbonized 1wt.% of Ag-PI composite film with hatch distance of 25 $\mu$ m and input pulse energy of 3 $\mu$ J. a) Processed with a pulse repetition rate of 200KHz b) Processed with a pulse repetition rate of 100KHz .....	15
Figure 9: Cross-sectional image of three samples with 1mm of laser scan on PI for pulse repetition rate (a) 200KHz (b) 100KHz and (c) 67KHz with hatch distance 25 $\mu$ m .....	16
Figure 10: Optical microscopic image of ultrafast laser processed carbonized 1wt.% of Ag-PI composite film with hatch distance of 50 $\mu$ m and input pulse energy of 3 $\mu$ J. a) Processed with a pulse repetition rate of 200KHz b) Processed with a pulse repetition rate of 100KHz .....	17
Figure 11: SEM image of pulsed laser carbonized (a) 1wt.% (b) 5wt.% silver in PI composite ...	18
Figure 12: EDS graph of carbonized 5wt.% silver in PI composite with hatch distance of 25 $\mu$ m, laser energy 3 $\mu$ J .....	18
Figure 13: Different wt.% of Ag in PI composite film and resistance relationship graph for 200KHz, 100KHz, and 67KHz pulse repetition rate (PPR).....	20
Figure 14: Change in resistance with the laser scan number of the carbonized pattern on Ag-PI composite film .....	21
Figure 15: Yb-fiber continuous wave laser treated carbonized PI in Ar gas environment with laser energy .....	22

Figure 16: Optical microscopic image of (a) pure PI and (b)Ag-PI composite treated with laser energy  $5.21\text{J}/\text{mm}^3$  .....23

Figure 17: Yb-fiber continuous wave laser treated sample by laser energies  $5.21\text{J}/\text{mm}^3$   $3.91\text{J}/\text{mm}^3$ ,  $3.13\text{J}/\text{mm}^3$ , and  $2.60\text{J}/\text{mm}^3$  in Ar environment .....24

Figure 18: SEM image of pulsed laser and continuous wave carbonized PI .....24

Figure 19: Wt.% of Ag in PI vs resistance for a different laser energy of CW laser.....25

## CHAPTER I

### INTRODUCTION

The demand for printed electronics that is flexible, compact, and more effective is expanding day by day. Conductive circuits on flexible substrates are attracting research interest in the areas of wearables, biomedical, and energy harvesters. A new method for producing functional nanocarbon on flexible substrates is the local carbonization of commercial polymers using lasers, such as polyimide. Due to its superior thermal stability up to 673K and greater insulating properties, PI is a very alluring material in the microelectronic and aerospace industry. In recent years, carbonizing polyimide (PI) through direct laser writing (DLW) has gained attention in the field of printed electronics due to its straightforward one-step process of inscribing conductive patterns in comparison to other mainstream printing techniques like photolithography, inkjet, and screen-printing. This discovery immediately attracted the attention of researchers from a variety of disciplines in investigating and inventing diverse applications employing direct laser writing on polyimide flexible electrodes, (Biswas et al., 2020; Farid et al., 2020; Qin et al., 2000; Rahimi et al., 2016a) various sensors, (Cheng et al., 2016; Fenzl, Nayak, Hirsch, Otto, et al., 2017; Jeong et al., 2019; Manuscript, 2018) supercapacitors, (Li et al., 2016; Wan et al., 2021) and so on.

The growing interest in fabricating laser carbon-based devices makes it essential to tune the laser

process parameters. For the patterning of carbon microelectrodes, laser pyrolysis has been proposed as a new approach (Fenzl, Nayak, Hirsch, Wolfbeis, et al., 2017; Mamleyev et al., 2019). Under ultraviolet laser irradiation, the electric conduction of a non-conductive PI substrate can be raised 15 to 16 times (Ball & Sauerbrey, 1994; Schumann et al., 1991). The irradiated sites are mostly made up of C-C bonds (Gu, 1993). The basic mechanism for laser pyrolysis is photothermal actions caused by laser irradiation. The photonic energy is transformed into heat when photons are absorbed by the polymer. The laser beam has a high intensity, and the polymer has a low heat conductivity, resulting in a big temperature gradient in a small zone (In et al., 2015; Science et al., 1989). This process is very fast, and the heating is concentrated in a precise area. Thus, microscale carbon patterning is enabled by scanning a polymer film with a laser beam, while the unaffected polymer area remains intact (In et al., 2015; Kim et al., 2019). Although a PI surface's electrical conductivity can be considerably improved by laser irradiation, there is still much room for improvement in terms of creating electrodes. The photo-thermal and photodegradation mechanisms have been comprehensively investigated by researchers for suitable laser-induced carbonization. The laser irradiation variables for the development of the carbon structure in the polyimide surface must be well suited for practical application in order to achieve induced conductivity.

In this study, polyimide film was prepared from polyimide resin in granulate. The reason for employing PI resin instead of the more common and commercially available polyimide film, Kapton tape, is that this resin provides more flexibility for internal modification of the prepared film. In order to adjust the amount of laser energy deposited on PI film, laser process parameters like hatch distance and pulse repetition rate were changed. A modification to the PI film was made by incorporating silver strands in addition to optimizing the laser process parameters to

improve conductivity and stability. Silver strands are more affordable than silver pastes or inks because less silver is required to achieve the same level of conductivity as is required for traditional silver particles or flakes. This is because of the exceptional structure of silver strands. The electrical conductivity of modified carbonized PI film was investigated for different laser process parameters.

For a better understanding of the effect of laser process on Ag-PI composite we conducted another study in a controlled environment. We proceed the carbonization in a closed Ar gas environment to reduce the effect of oxygen on printed pattern on modified Ag-PI substrate. Controlled environment processing showed promising direction for processing Ag-PI composite film.

## CHAPTER II

### BACKGROUND

#### **Direct Laser Writing and Carbonization of PI**

Direct laser writing technology has become an essential tool for the processing of a wide range of materials, including metals, polymers, ceramics, and others, in order to manufacture and create a variety of functional devices. Its precision, versatility, and capability to pattern without the use of a mask have this technique a powerful alternative to other methods.(Biswas et al., 2020; Debroy et al., 2018; Dorin et al., 2017; Maruo & Saeki, 2008) Laser technology is environment friendly, contactless, and easy to control with a higher repeatability rate. In comparison with the conventional method for carbonizing polymer direct laser writing carbonization (DLWc) offers a more adaptable, and tightly regulated means of producing carbonized structures in a regular environment. (Ye et al., 2019) The carbon structures developed by DLW have a number of benefits, including a large surface area, great thermal constancy, and outstanding electrical conductance. Materials with length scales ranging from nanometers to meters can be processed using a wide variety of laser powers and contact times. With optimized laser process parameters, a laser beam is able to print carbon patterns on PI by altering the property of PI. Computer-controlled laser system can create any pattern with the movement of a platform when the laser spot is positioned on it. The period between fundamental research of

material to start industrial production has been greatly shortened due to the excellent scalability of laser writing. To fully utilize the DLW method, it is crucial getting a solid knowledge of the processing and construction relations.

Schumann et al. used a 248 nm KrF laser to accomplish the novel idea of laser carbonization of PI in 1991, resulting in a conductivity increase of up to 15 times that of pure PI.(Schumann et al., 1991) Additionally, more research is going through to create carbon on polyimide with improved electrical conductivity employing ultra-violet light in the form of a continuous wave or a femtosecond pulse.(Maruo & Saeki, 2008; Palm, 2012; Wang et al., 2017) In a different study, the laser-irradiated PI surface was covered with a metal ion solution to create a surface composite of metal and carbonated structure in order to increase electrical conductivity. (Rahimi et al., 2016b) A significant order of improvement would be seen in the conductivity of PI that has been laser treated and coated with Ag ion solution. This results from an abundance of silver nanoparticles attached to porous carbonated structures through photoreduction. But in this process the simplicity of laser processing gets hampered. There are still space to improve in the field of laser carbonized structure in polymer and scope to contribute in those areas.

### **Research Question**

- How do the laser process parameters like pulse energy, pulse picker divider, and laser scan hatch distance have effect on the electrical conductivity of the printed patterns?
- How to improve the electrical conductivity of laser-written structures with better stability?

- In the case of modified PI composite how carbon structures are affected by the environment?

### **Modification of Polyimide Film**

In literature, there are a couple of different approaches to modifying the polyimide. Polyimide is electrically non-conductive in nature. Laser carbonization allows the making of a conductive line on polyimide by converting the material into carbon through the pyrolysis process. For further improvement of the conductivity, adding silver strands in polyimide film is an approach. Silver is a well-established conductive material and used in electrodes for its low resistivity properties. When silver strands in polyimide film should give additional conductive property along with the carbonized line which ultimately help to progress the overall conductivity of the LDW lines. Silver strands added into the polyimide solution to achieve inner modification to improve the conductivity. When subjected to thermal and electrical stress, silver strands' distinctive one-dimensional nanostructure makes the substance exceptionally strong and stable. Silver strands are more cost effective as compared to silver pastes or inks as to attain the same amount of conductivity less silver is needed for silver strands than the traditional silver particle or flakes due to its open structure. The modified silver-polyimide composite film would be electrically non-conductive before any laser treatment. After laser direct writing the patterns will act as an electrode and improve overall conductivity as silver nanowires will improve the inner electrical properties of the composite film. Those nanowires will help filling the cracks which are formed through the laser pyrolysis on polyimide film. This inner modification will offer better bonding between polymer and nano wire and provide improved electrical conductivity. Different wt.% of nanoparticle in polyimide film was tested to achieve the best output in its electrically conductive property.



## CHAPTER III

### METHODOLOGY

#### Material Preparation

##### Pure Polyimide

The fully imidized polyimide resin in granulate form (TECAPOWDER P84, SG, inventory# 58698-66-1) from Engineer Sintimid GmbH, Austria was used to prepare PI solution. The dipolar aprotic solvent, 1-Methyl-2-pyrrolidinone (NMP) was the solvent here to dissolve the granulate PI and make the solution form. 15 wt.% of polyimide resins were added into the NMP for 24 hours on a mixer at low speed.

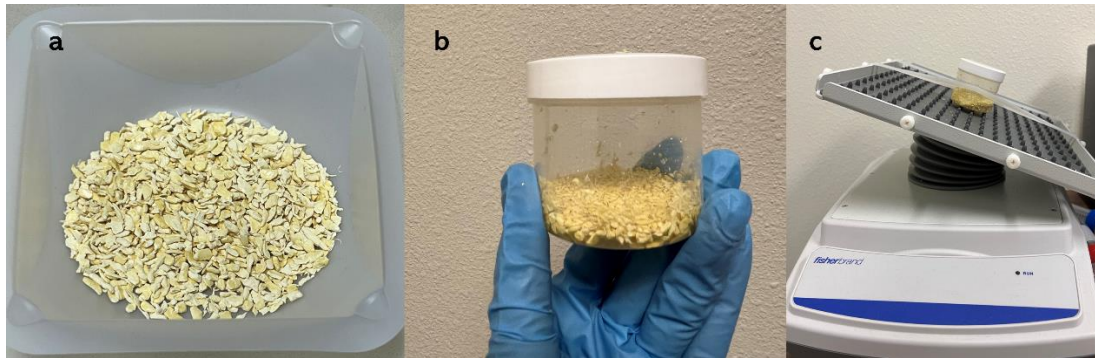


Figure 1-(a) Granulate PI resin. (b)15wt.% of PI in the solvent NMP (c) Dissolving PI in the NMP at the low-speed mixer.

Figure 2 shows the PI in liquid form after 24 hours of mixing. To make the film from the solution dip-coating procedure was used and then cured at room temperature according to

specification sheet. The dip-coated PI films were dried in laboratory conditions to prepare the fully cured PI substrates. Digital calipers were used to measure the thickness of the prepared PI film, which was around 250-300 $\mu\text{m}$ .

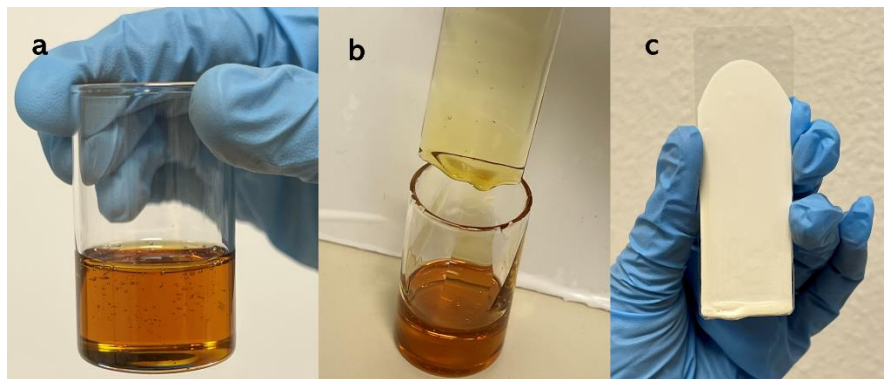


Figure 2- (a) Polyimide resin dissolved in NMP after 24hours of mixing at low-speed. (b) Dip coating of glass slide into the PI solution. (c) Fully cured PI film.

### **Silver strands-Polyimide composite film**

For further investigation pure polyimide solution were modified by adding different weight percentage of silver strands from NanoCnet. Silver strands is a one-dimensional distinctive type of nanostructure. Along with pure PI film, four more silver strands/polyimide composite film were prepared by adding different wt.% of silver strands into the polyimide solution. We investigated 0.5wt.%, 1wt.%, wt.2% and 5wt% of silver strands/polyimide composite film for our studies.

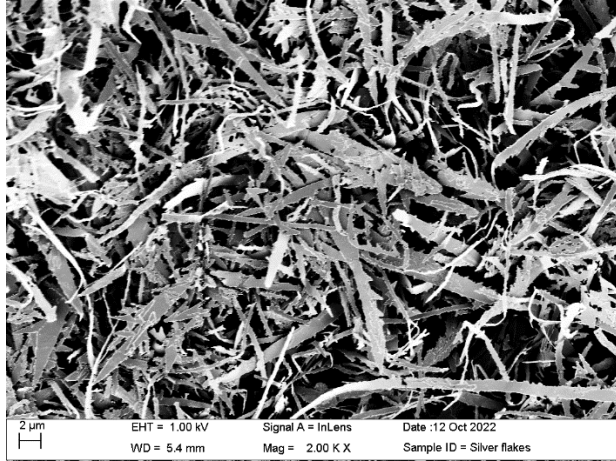


Figure 3- SEM image of silver strands.

For making the composite film first step was dispersing the silver strands into the NMP solvent. For proper dispersing, the silver strands were mixed first in the NMP using a homogenizer mixer for 10 minutes. It helped the silver strands to fully dispersed in the solvent. Then the granulate polyimide resins were added into the silver strands-NMP solution to prepare our Ag-PI composite solution. The solution was kept on a slow speed mixer for 24hours to fully dissolve the polyimide into the solution. After that to ensure proper dispersion of silver strands into the polyimide solution we used Hauschild Speed Mixer. The solution was kept in the mixer for 5minutes at 2500rpm. For preparing the silver strands/PI composite film from the composite solution the dip-coating method was employed to create the film, which was then cured at room temperature.

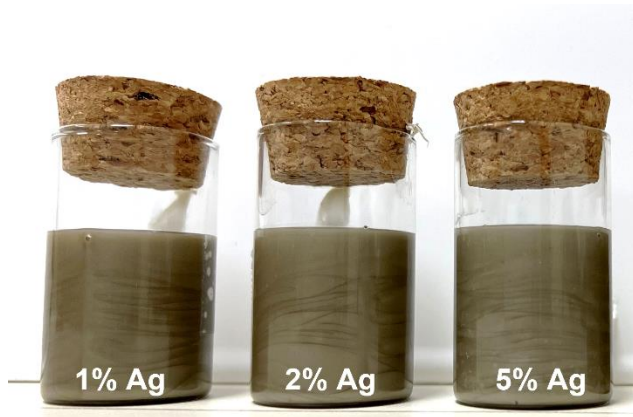


Figure 4- Image of Ag-PI composite solution for different wt.% of silver strands.

In fig. 4. We can see the Ag-PI composite solution prepared with different wt.% of silver strands.

To get better mixing this solution were mixed three times using different mixer.

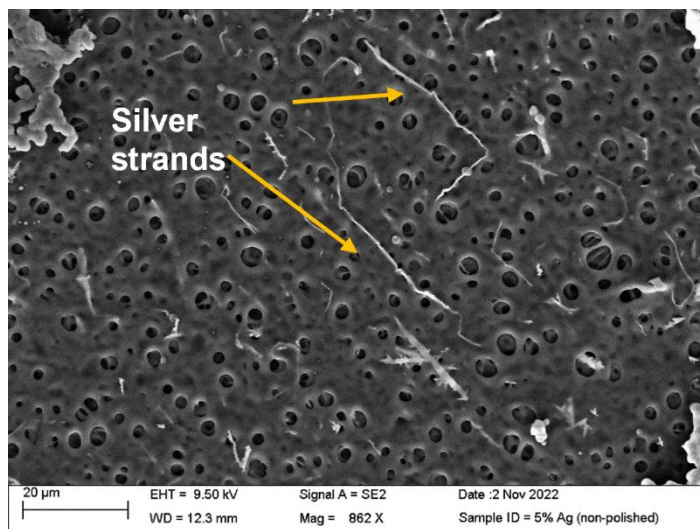


Figure 5-SEM image of 5wt.% Ag-PI composite film.

In figure 5 dispersed silver strands are visible on the surface of the film. Some portions of the strands are buried in the PI film.

## Laser Processing

### Ultra-fast laser carbonization

A commercially available ultrafast pulsed Nd:YAG laser (a Spirit® laser from Spectra-Physics), operating at a center wavelength of 1040 nm, pulse duration of 500 fs, and maximum pulse energy of 40  $\mu$ J at 200 kHz was used to perform the experiments. With an integrated acousto-optic-modulator, the basic repetition rate can be divided by an integer value. Spirit® provides laser parameter optimization for femtosecond lasers used in high-precision manufacturing of polymers, thin metals, and a variety of other materials.

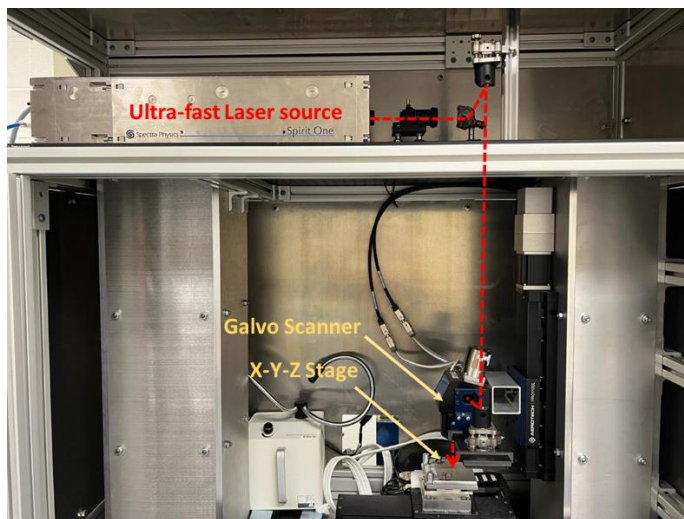


Figure 6-Ultrafast laser system used for carbonization.

To modify the electrical properties of PI film, ultrafast laser light was used to selectively carbonize the film. The threshold energy needed to start the pyrolysis process in order to carbonize the polyimide film should be delivered by the laser beam, which can be done at various laser energies and scanning rates. Different laser energies and scanning speeds were initially investigated. Excess thermal energies result in cutting through the substrate or damage the substrate while low thermal energies will be unable to carbonize the polymer effectively. All

the tests were conducted using a laser energy of  $3\mu\text{J}$  and a scanning speed of  $10\text{mm/s}$ , which had significant effects on the carbonization of PI. To optimize the outcomes, the hatch distance of the scanned lines was varied. Hatch distances of  $25\mu\text{m}$  and  $50\mu\text{m}$  where the laser beam spot size was  $30\mu\text{m}$ . The basic pulse repetition rate was varied selecting different pulse picker divider (PPD). The PPDs of 1, 2, and 3 were considered to alter the total laser energy deposition onto the PI substrates for printing conductive paths. Pulse repetition rates were  $200\text{KHz}$ ,  $100\text{KHz}$  and  $67\text{KHz}$  for the tests. Straight lines were scanned by laser irradiation on polyimide and all the conductive patterns were  $10\text{mm}$  in length with  $1\text{mm}$  in width. For consistent result a couple of lines were printed for single process parameters. The morphologies of the conductive lines on PI substrate were investigated using an optical microscope and a scanning electron microscope (SEM) and the resistance were measured using a source-meter from Keithley. The data of resistance of each conductive path were measured multiple times to get a reliable value.

### **Continuous-wave laser carbonization**

Direct laser irradiation on the polyimide film by was conducted by maximum power  $400\text{W}$  Yb-fiber continuous wave laser with focus diameter  $100\mu\text{m}$ . To prevent oxygen interaction, processing with a continuous wave laser was done in an Ar gas atmosphere. For getting the proper carbonization process parameters like laser's power and speed have a significant impact on the heat created during the process, as well as the microstructure and surface qualities of the resultant carbon. The optimal laser energy was determined by varying the scanning speed while keeping the power constant at  $10\text{W}$ , and the distance between the lines was held constant at  $80\mu\text{m}$  for all testing. Experiments were carried out at laser scanning speed of  $300\text{mm/s}$ ,  $400\text{mm/s}$ ,  $600\text{mm/s}$ ,  $800\text{mm/s}$ ,  $1000\text{mm/s}$  and  $1200\text{mm/s}$ . By maintaining the power

and hatch distance constant while varying the scanning speed, as shown in the table, laser energy adjusts.

Table 1- Process parameters for CW laser system.

Trial	Speed in mm/s	Laser Energy in J/mm <sup>3</sup>
1	300	10.42
2	400	7.81
3	600	5.21
4	800	3.91
5	1000	3.13
6	1200	2.60

## CHAPTER IV

### RESULTS AND FINDINGS

#### Pulsed Laser Processed

Figure 7 shows the laser carbonized conductive lines on the PI substrates. Pulse repetition rate was used to control the laser energy deposition in the PI substrates. When higher pulse repetition rate values were used, dominant carbonization was observed as shown in Fig.7. For lower pulse repetition rate, fewer pulses were allowed to reach the PI substrate, thus reducing the amount of laser energy into the substrate. Hence, the laser carbonization was less prevalent as carbonized lines appeared lighter in color shown in Fig. 7.

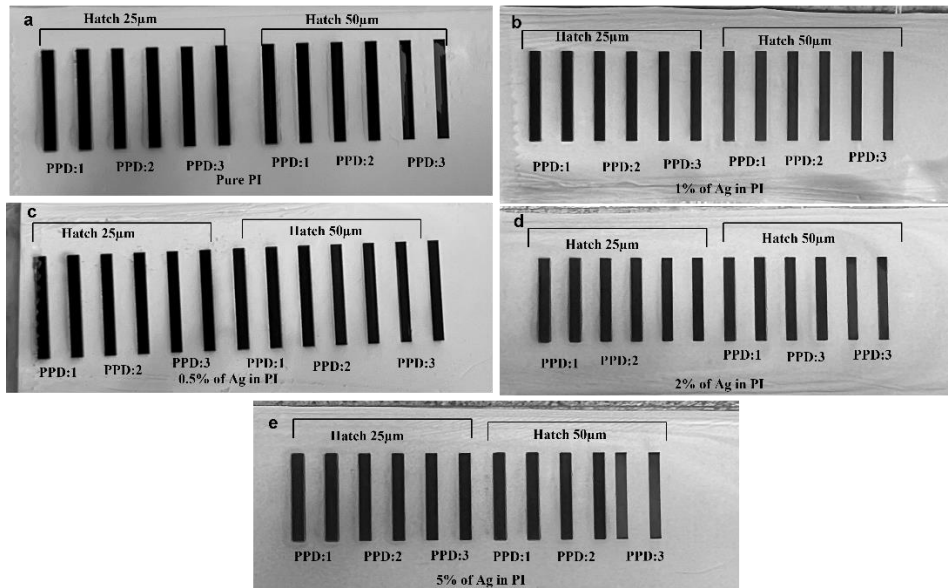


Figure 7-Femtosecond pulsed laser processed carbonized pattern by varying process parameters on different wt.% of silver-PI composite film. (a) Pure PI film. (b) (c) (d) and (e) are 0.5%, 1%,



2% and 5% of Ag-PI composite film

Figure shows 1mm by 10mm carbonized patterns for different process parameters. Pulse picker divider (PPD) are used to control the pulse repetition rate. Higher PPD blocks more pulses which decrease the pulse repetition rate. As shown in Fig. 7, in addition to variable PPD, three different hatch distances of laser scanning were used to control the delivery of laser energy into the PI substrate. Two different hatch distance were used to here, 25 $\mu$ m and 50 $\mu$ m to control the laser energy along with pulse repetition rate.

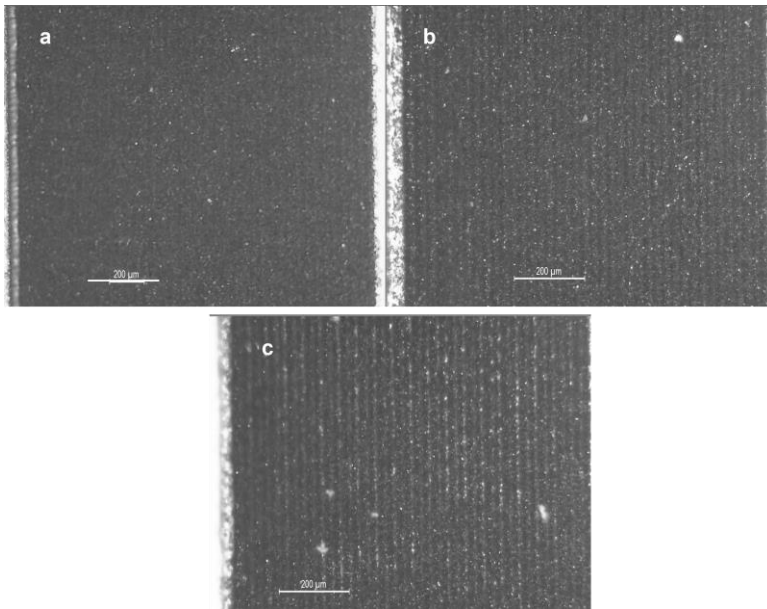


Figure 8-Optical microscopic image of ultrafast laser processed carbonized 1wt.% of Ag-PI composite film with hatch distance of 25 $\mu$ m and input pulse energy of 3 $\mu$ J. a) Processed with pulse repetition rate of 200KHz b) Processed with pulse repetition rate of 100KHz.

In figure 8, for an input pulse energy of 3 $\mu$ J, the impact of pulse repetition rate of 200KHz, 100KHz and 67KHz are shown in the optical microscope images of Fig.(a), (b) and (c) respectively. Evidence of higher carbonization was observed for which is also later supported by the lower conduction resistance measured during the testing.

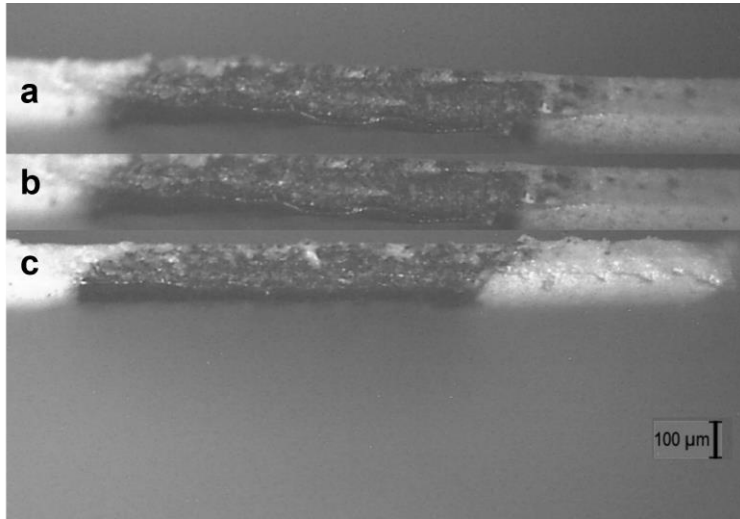


Figure 9-Cross sectional image of three samples with 1mm of laser scan on PI for pulse repetition rate (a) 200KHz (b) 100KHz and (c) 67KHz with hatch distance 25 $\mu$ m.

From Figure 9 we can see that for higher pulse repetition rate there is a trend of increasing the carbonized area more than the laser scan area. Because of the higher energy than the other two (a) has more carbonized are than (b) and (c). This provides proof that increasing laser energy causes more carbonization on PI which helps to decrease the resistance.

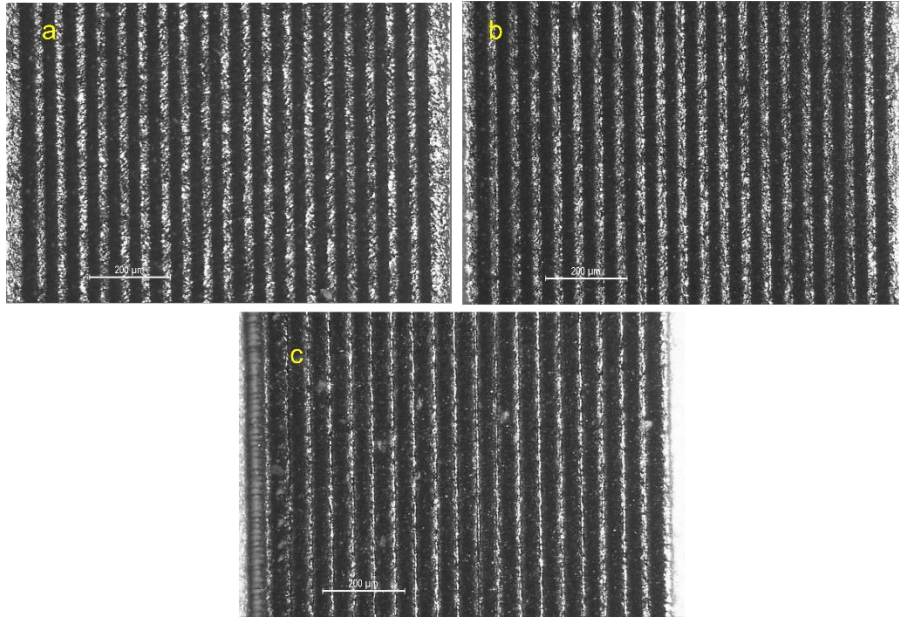


Figure 10-Optical microscopic image of ultrafast laser processed carbonized 1wt.% of Ag-PI composite film with hatch distance of 50 $\mu$ m and input pulse energy of 3 $\mu$ J. a) Processed with pulse repetition rate of 200KHz b) Processed with pulse repetition rate of 100KHz

As the hatch distances are increased in this sample parameter, the grooves become more noticeable in Fig. 10. As can be seen, grooves are deeper at higher pulse repetition rates than for lower pulse repetition rates. This is due to the fact that larger pulse at a time allows for greater energy deposition on a single point.

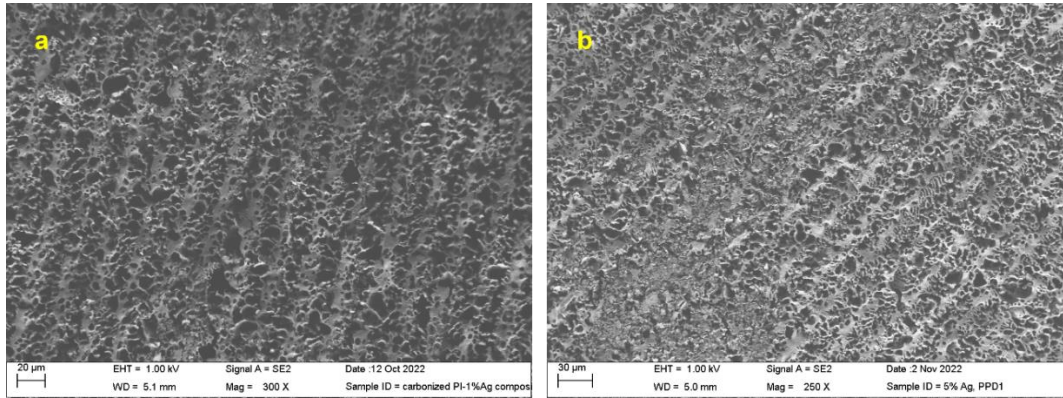


Figure 11-SEM image of pulsed laser carbonized (a)1wt.% (b) 5wt.% silver in PI composite. Figure 11 shows the SEM images of the laser carbonized PI substrate when processed with pulse energy of 3  $\mu$ J, PPD of 1, and hatch distance of 25  $\mu$ m. The grooves are visible along the laser scan paths along with carbonization of PI in between hatches. This explains why the lack of sufficient carbonization in case of larger hatch distance resulted in relatively higher electrical resistance values, as seen in table 2. The energy dispersive X-ray spectroscopy (EDS) shown in Fig. 12 confirms substantial presence of carbon in the laser modified area. It also shows the presence of Ag in the treated area. Oxygen was used for sputtering which is also in the graph.

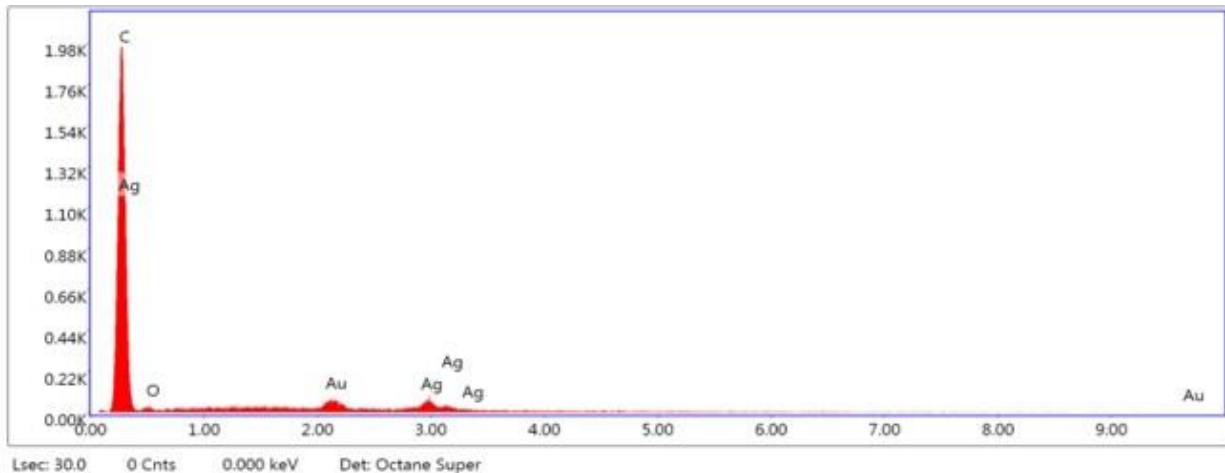


Figure 12-EDS graph of carbonized 5wt.% silver in PI composite with hatch distance of 25 $\mu$ m, laser energy 3 $\mu$ J.

Table 2-Resistance value for 1×10 mm carbonized lines at speed 10m/s and laser energy of 3μJ.

Wt.% of Ag in PI	Hatch distance between single scan	Resistance in KΩ for Pulse Repetition Rate of 200KHz	Resistance in KΩ for Pulse Repetition Rate of 100KHz	Resistance in KΩ for Pulse Repetition Rate of 67KHz
0%	25μm	0.28	0.68	1.2
	50 μm	0.38	0.98	5.68
0.5%	25 μm	0.30	0.67	1.3
	50 μm	0.28	1.12	9.5
1%	25μm	0.30	0.66	1.2
	50 μm	0.30	1.20	3.5
2%	25μm	0.35	0.72	1.37
	50 μm	0.36	1.06	-
5%	25μm	0.33	1.01	2
	50 μm	0.39	1.9	-

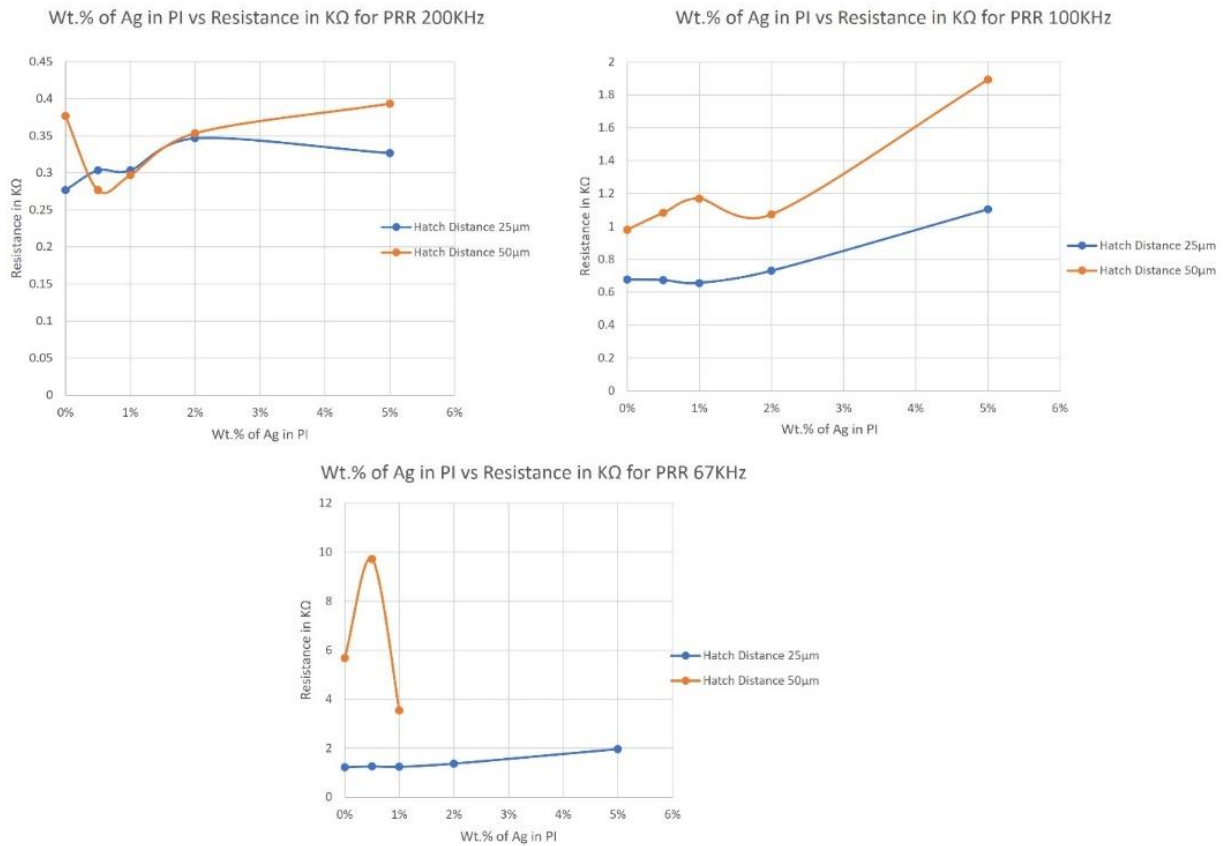


Figure 13-Different wt.% of Ag in PI composite film and resistance relationship graph for 200KHz, 100KHz and 67KHz Pulse repetition rate (PPR).

In the figure 13, different wt.% of Ag in PI composite film and resistance relationship graph for 200KHz, 100KHz and 67KHz Pulse repetition rate (PPR) is shown. The orange line stands for hatch distance of 50 μm where blue line stands for hatch distance 25 μm. It is visible that for higher hatch resistance is higher and for smaller hatch distance resistance value is also lower.

When the silver content in the composite film is raised, all three graphs indicate an upward trend for resistance, however there are some inconsistencies. The oxidation of silver strands during processing is thought to be the reason why. The experiments were carried out in a setting with

ambient oxygen. When in contact with oxygen, silver oxidizes relatively quickly. Therefore, due to the non-conductive nature of oxides, the resistance value is greater for more percentage of silver.

Table 3-Resistance value for different number of laser scanning line with hatch 25 $\mu$ m.

% of Ag in PI	R for single scan	R for width 0.125mm	R for width 0.25mm	R for width 0.5mm
0.50%	10	2	1.1	0.55
1%	10.63	2.1	1.1	0.65
2%	13.7	2.5	1.32	0.68
5%	22	2.9	1.41	0.7

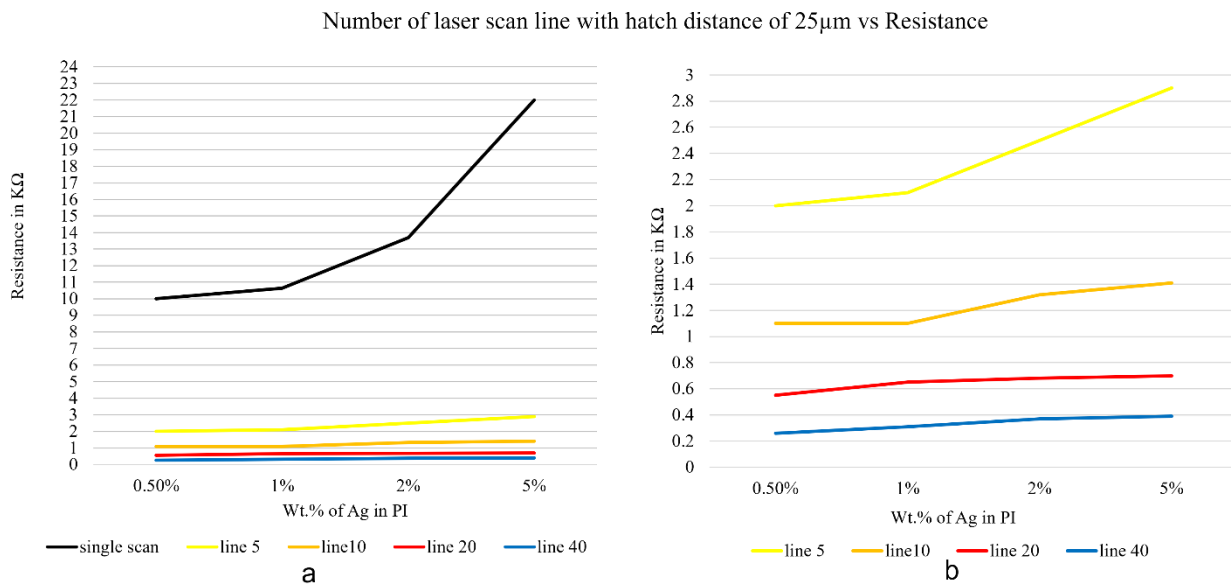


Figure 14-Change in resistance with the laser scan number of the carbonized pattern on Ag-PI composite film.

For single scan line, in figure 14(a), we can see that the resistance value is going sharply upward when the percentage of Ag in the composite film is higher. This is due to the fact that silver oxide dispersion increases with increasing silver content. It hampers the flow of electricity and

causes a sharp rise in resistance. However, as the number of scan lines rises, more carbonized area is produced, aiding in the avoidance of such blockages and providing a conduit for the passage of electricity. As a result, the increase in resistance is less dramatic for multiple scan lines than for single scan line, which is clear in figure 14(b).

### CW-Laser processing in Ar gas environment

Other studies employing a Yb-fiber continuous wave laser in a controlled Ar gas environment were done to verify the impact of oxidation on the resistance value. Another set of samples that were laser-treated in an Ar gas atmosphere are presented in the figure.

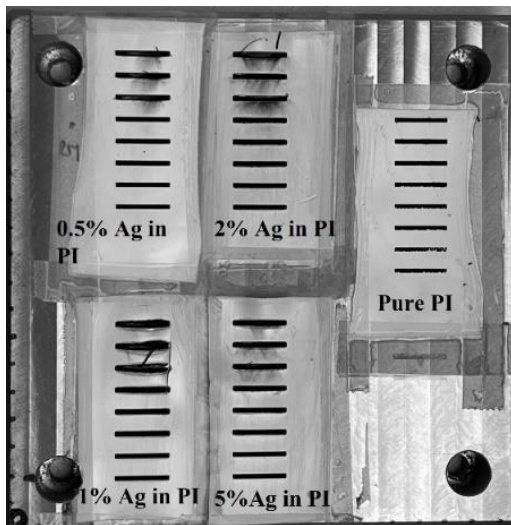


Figure 15-Yb-fiber continuous wave laser treated carbonized PI in Ar gas environment with laser energy.

Here, laser energy  $10.42\text{J}/\text{mm}^3$   $7.81\text{J}/\text{mm}^3$   $5.21\text{J}/\text{mm}^3$  were deposited to alter the polyimide film into carbon. For higher energy it can be seen that the Ag-PI composite films got damaged.

However, it is worth noting that pure PI is able to withstand with that amount of heat and



carbonized properly power. It is because metal is more likely to conduct heat and absorbs more heat than the polymer which affects the composite films. For pure PI  $5.21\text{J}/\text{mm}^3$  energy was not enough to carbonize entirely. The laser's power and speed have a significant impact on the heat created during the process, along with the microstructure and surface qualities of the resultant carbon. In figure 16(a), we can see the lack of carbonization of pure PI treated with laser energy  $5.21\text{J}/\text{mm}^3$  in the optical microscopic image. In 16(b) for the same power Ag-PI composite film was carbonized properly without any damage.

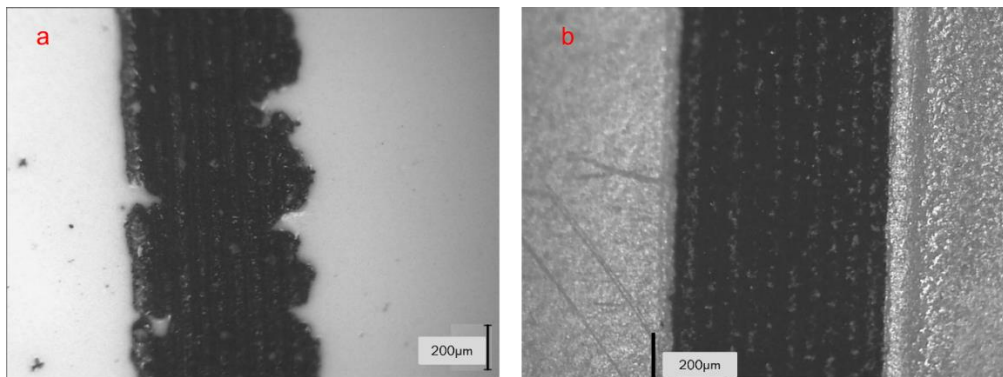


Figure 16- Optical microscopic image of (a) pure PI and (b) Ag-PI composite treated with laser energy  $5.21\text{J}/\text{mm}^3$ .

Another set of process data were studied to figure optimum laser energy to carbonize Ag-PI composite film. Laser energy  $5.21\text{J}/\text{mm}^3$ ,  $3.91\text{J}/\text{mm}^3$ ,  $3.13\text{J}/\text{mm}^3$  and  $2.60\text{J}/\text{mm}^3$  were tested to optimize the energy and all of these values of energies were able to carbonize the Ag-PI composite film without damaging them. We also can see that the patterns were carbonized properly. By increasing the scanning speed and keeping the other laser parameters constant, power at 10W and hatch distance at .08mm, these energies were attained.

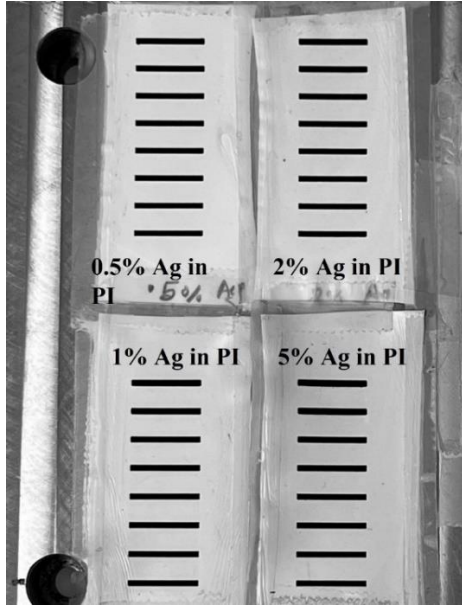


Figure 17-Yb-fiber continuous wave laser treated sample by laser energies 5.21J/mm<sup>3</sup> 3.91 J/mm<sup>3</sup>, 3.13 J/mm<sup>3</sup> and 2.60 J/mm<sup>3</sup> in Ar environment.

From the figure 17 it is visible that composite PI film is able to carbonize at a lower energy of laser than the pure PI. Laser energies 5.21J/mm<sup>3</sup>, 3.91 J/mm<sup>3</sup>, 3.13 J/mm<sup>3</sup> and 2.60 J/mm<sup>3</sup> were enough to carbonize the Ag-PI composite film.

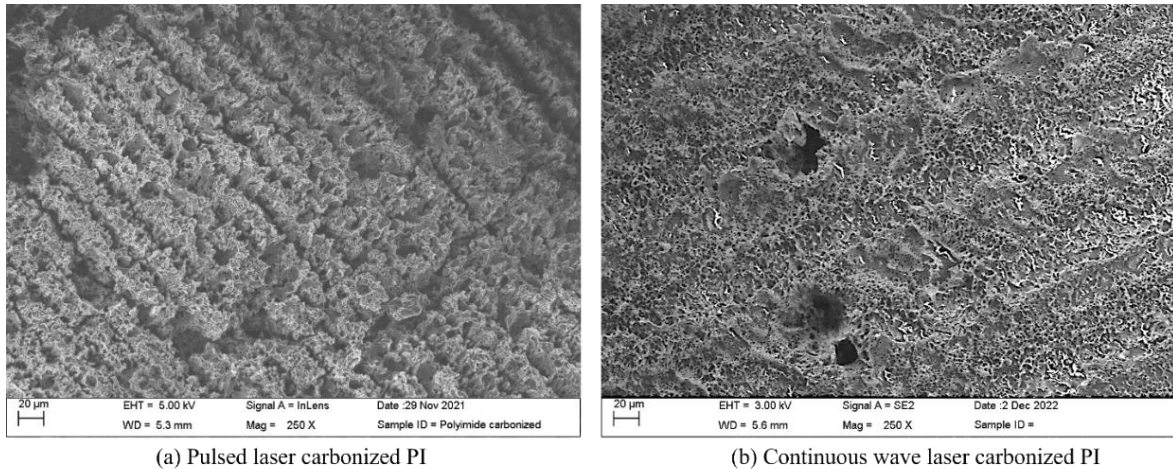


Figure 18-SEM image of pulsed laser and continuous wave carbonized PI.

In fig. 18, From the SEM image it is visible that the pulse laser created deeper grooves where CW laser carbonized the film more uniformly. This is because for pulsed laser energy is deposited on a single point much more precisely.

Table 4-Resistance value of  $1 \times 10$  mm carbonized lines at hatch distance of 0.08mm and power 10W.

Wt.% of Ag in PI	Resistance Value in $K\Omega$ for Laser energy $5.21 \text{ J/mm}^3$	Resistance Value in $K\Omega$ for Laser energy $3.91 \text{ J/mm}^3$	Resistance Value in $K\Omega$ for Laser energy $3.13 \text{ J/mm}^3$	Resistance Value in $K\Omega$ for Laser energy $2.6 \text{ J/mm}^3$
0.5%	2.45	7.52	16.17	32.62
1%	2.36	8.60	20.13	32.87
2%	2.31	7.91	17.82	33.1
5%	1.3	3.88	13.2	32.20

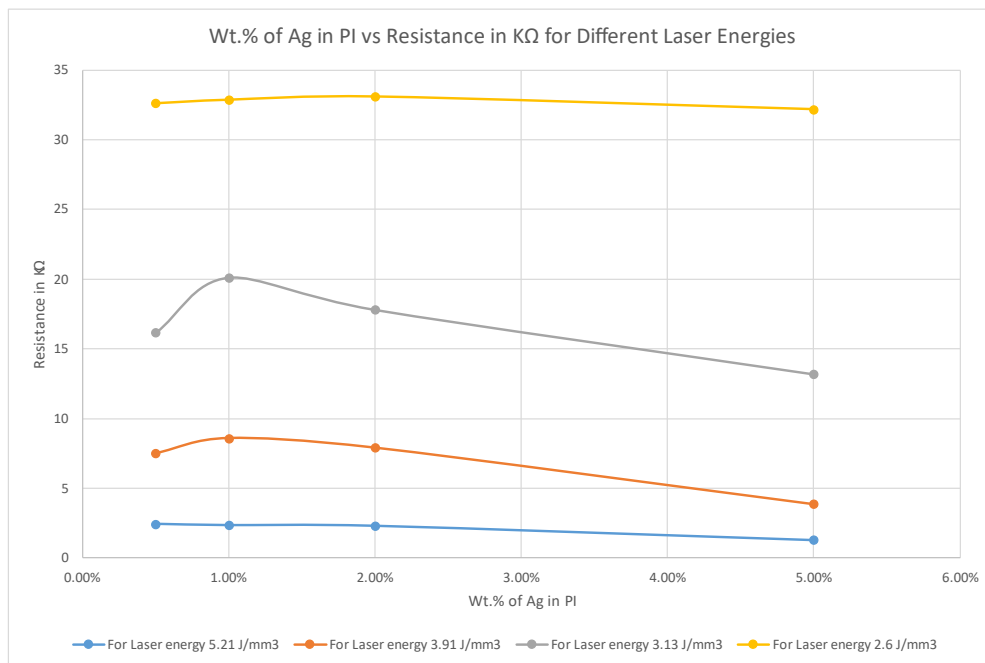


Figure 19-Wt.% of Ag in PI vs resistance for different laser energy of CW laser.

In the figure, all the graphs show a downward trend of resistance value for higher Ag content in the Ag-Pi composite film. These experiments were conducted in a controlled Ar gas environment. Because of controlled environment there were no oxygen to oxidize silver strands. Which helps the silver strand to contribute to the overall conductivity of the laser printed patterns. From the graph we can say that modifying PI film by adding silver strands has contribution of improving conductivity of carbonized circuits.

## CHAPTER V

### CONCLUSION, LIMITATIONS, & FUTURE DIRECTION

In summary, we studied ultra-fast laser-induced carbonization of polyamide to selectively enhance electrical conductivity within the PI substrate for printed electronics applications. Controlled deposition of laser energy was found to be the key parameter to enhance the electrical conductivity of the PI substrate. For further improvement, silver strands polyimide composite films were studied for laser carbonization method. However, due to oxygen environment silver strands were turned into silver oxide which is non-conductive and significantly affected in conductivity of those carbonized circuits. To confirm the effect of the oxygen for composite film further laser carbonization was conducted in Ar gas environment to reduce oxidation of the silver strands. Laser carbonization in controlled environment showed promising result of improvement of conductivity of the carbonized patterns. The laser's power, fluence, speed, and pyrolysis environment, in addition to its wavelength, have a significant impact on the electrical property of the carbonized lines as well as the microstructure and surface characteristics of the carbon that is produced. This result shows great potential for laser-induced conductive circuits for the printed electronics industry. The next step in our research is to increase the conductivity of the modified Ag-polymer composite film by processing with pulsed laser in controlled environment. Better comparison can be achieved between pulsed laser processing and continuous wave laser processing. Furthermore, laser treated composite film will be tested in flexible electronics and sensor application.

## REFERENCES

- Ball, Z., & Sauerbrey, R. (1994). Lowering of the conduction threshold by carbon fiber formation in KrF excimer laser irradiated polyimide. *Applied Physics Letters*, 65(4), 391–393. <https://doi.org/10.1063/1.112342>
- Biswas, R. K., Farid, N., O'Connor, G., & Scully, P. (2020). Improved conductivity of carbonized polyimide by CO<sub>2</sub> laser graphitization. *Journal of Materials Chemistry C*, 8(13), 4493–4501. <https://doi.org/10.1039/c9tc05737d>
- Cheng, C., Wang, S., Wu, J., Yu, Y., Li, R., Chen, J., Feng, G., Lawrie, B. J., & Hu, A. (2016). *Bisphenol-A sensors on polyimide fabricated by laser direct writing for on-site river water monitoring at attomolar concentration*. <https://doi.org/10.1021/acsami.6b03743>
- Debroy, T., Wei, H. L., Zuback, J. S., Mukherjee, T., Elmer, J. W., Milewski, J. O., Beese, A. M., Wilson-heid, A., De, A., & Zhang, W. (2018). *Progress in Materials Science Additive manufacturing of metallic components – Process , structure and properties*. 92, 112–224. <https://doi.org/10.1016/j.pmatsci.2017.10.001>
- Dorin, B., Parkinson, P., & Scully, P. (2017). Direct laser write process for 3D conductive carbon circuits in polyimide. *Journal of Materials Chemistry C*, 5(20), 4923–4930. <https://doi.org/10.1039/c7tc01111c>
- Farid, N., Connor, G. O., & Scully, P. (2020). *Improved conductivity of carbonized polyimide by CO<sub>2</sub> laser graphitization*. February. <https://doi.org/10.1039/C9TC05737D>
- Fenzl, C., Nayak, P., Hirsch, T., Otto, S., Alshareef, H. N., & Baeumner, A. J. (2017). *Laser-scribed graphene electrodes for aptamer-based biosensing*. *Laser-scribed graphene electrodes for aptamer-based biosensing*.
- Fenzl, C., Nayak, P., Hirsch, T., Wolfbeis, O. S., Alshareef, H. N., & Baeumner, A. J. (2017). Laser-Scribed Graphene Electrodes for Aptamer-Based Biosensing. *ACS Sensors*, 2(5), 616–620. <https://doi.org/10.1021/acssensors.7b00066>
- Gu, X. J. (1993). Raman spectroscopy and the effects of ultraviolet irradiation on polyimide film. *Applied Physics Letters*, 62(13), 1568–1570. <https://doi.org/10.1063/1.108643>
- Highly Sensitive , Stretchable , and Wash- Durable Strain Sensor Based on Ultrathin Conductive Layer @ Polyurethane Yarn for Tiny Motion Monitoring*. (2016). <https://doi.org/10.1021/acsami.6b01174>

- In, J. Bin, Hsia, B., Yoo, J. H., Hyun, S., Carraro, C., Maboudian, R., & Grigoropoulos, C. P. (2015). Facile fabrication of flexible all solid-state micro-supercapacitor by direct laser writing of porous carbon in polyimide. *Carbon*, 83, 144–151. <https://doi.org/10.1016/j.carbon.2014.11.017>
- Jeong, S., Ma, Y., Lee, J., Je, G., & Shin, B. (2019). *Flexible and Highly Sensitive Strain Sensor Based on Laser-Induced Graphene Pattern Fabricated by*. 1–12.
- Kim, K. Y., Choi, H., Tran, C. Van, & In, J. Bin. (2019). Simultaneous densification and nitrogen doping of laser-induced graphene by duplicated pyrolysis for supercapacitor applications. *Journal of Power Sources*, 441(September), 227199. <https://doi.org/10.1016/j.jpowsour.2019.227199>
- Li, L., Zhang, J., Peng, Z., Li, Y., Gao, C., Ji, Y., Ye, R., Kim, N. D., Zhong, Q., Yang, Y., Fei, H., Ruan, G., & Tour, J. M. (2016). High-Performance Pseudocapacitive Microsupercapacitors from Laser-Induced Graphene. *Advanced Materials*, 28(5), 838–845. <https://doi.org/10.1002/adma.201503333>
- Mamleyev, E. R., Heissler, S., Nefedov, A., Weidler, P. G., Nordin, N., Kudryashov, V. V., Länge, K., MacKinnon, N., & Sharma, S. (2019). Laser-induced hierarchical carbon patterns on polyimide substrates for flexible urea sensors. *Npj Flexible Electronics*, 3(1). <https://doi.org/10.1038/s41528-018-0047-8>
- Manuscript, A. (2018). *Materials Chemistry C*. <https://doi.org/10.1039/C8TC00457A>
- Maruo, S., & Saeki, T. (2008). Femtosecond laser direct writing of metallic microstructures by photoreduction of silver nitrate in a polymer matrix. *Optics Express*, 16(2), 1174. <https://doi.org/10.1364/oe.16.001174>
- Palm, W. J. (2012). Wavelength and temperature dependence of continuous-wave laser absorptance in Kapton<sup>®</sup> thin films. *Optical Engineering*, 51(12), 121802. <https://doi.org/10.1117/1.oe.51.12.121802>
- Qin, Z., Huang, X., Wang, D., He, T., Wang, Q., & Zhang, Y. (2000). Formation of conducting layers on excimer-laser-irradiated polyimide film surfaces. *Surface and Interface Analysis*, 29(8), 514–518. [https://doi.org/10.1002/1096-9918\(200008\)29:8<514::AID-SIA895>3.0.CO;2-Q](https://doi.org/10.1002/1096-9918(200008)29:8<514::AID-SIA895>3.0.CO;2-Q)
- Rahimi, R., Ochoa, M., & Ziaie, B. (2016a). Direct Laser Writing of Porous-Carbon/Silver Nanocomposite for Flexible Electronics. *ACS Applied Materials and Interfaces*, 8(26), 16907–16913. <https://doi.org/10.1021/acsami.6b02952>
- Rahimi, R., Ochoa, M., & Ziaie, B. (2016b). *Direct Laser Writing of Porous-Carbon / Silver Nanocomposite for Flexible Electronics*. 1–7. <https://doi.org/10.1021/acsami.6b02952>

- Schumann, M., Sauerbrey, R., & Smayling, M. C. (1991). Permanent increase of the electrical conductivity of polymers induced by ultraviolet laser radiation. *Applied Physics Letters*, 58(4), 428–430. <https://doi.org/10.1063/1.104624>
- Science, A. S., This, C., The, C., & Publishers, E. S. (1989). *Influence of the Temperature on the Ion Beam Induced Conductivity of Polyimide*. 43, 218–223.
- Wan, Z., Chen, X., & Gu, M. (2021). Laser scribed graphene for supercapacitors. *Opto-Electronic Advances*, 4(7), 1–21. <https://doi.org/10.29026/oea.2021.200079>
- Wang, S., Yu, Y., Ma, D., Bridges, D., Feng, G., & Hu, A. (2017). High performance hybrid supercapacitors on flexible polyimide sheets using femtosecond laser 3D writing. *Journal of Laser Applications*, 29(2), 022203. <https://doi.org/10.2351/1.4983513>
- Ye, R., James, D. K., & Tour, J. M. (2019). *Laser-Induced Graphene : From Discovery to Translation*. 1803621, 1–15. <https://doi.org/10.1002/adma.201803621>



## BIOGRAPHICAL SKETCH

Ishrat Jahan Biswas was born in Bangladesh city of Rajshahi. Ishrat enrolled in Master of Science in Engineering program in the University of Texas Rio Grande Valley after graduating from the Shahjalal University of Science and Technology, Sylhet, Bangladesh in 2021. She completed her Master of Science degree in Manufacturing Engineering by December 2022. She is going to start her Ph.D. in Electrical and Computer Engineering in the Florida International University from January,2023. She can be reached at [ishratbiswas@gmail.com](mailto:ishratbiswas@gmail.com).